FLUORESCENCE AND THERMAL STUDY OF 3D METAL COMPLEXES CONTAINING HEXADENTATE SCHIFF BASE LIGAND

Carmen CRETU, Viorel SASCA, Elisabeta I. SZERB, Liliana CSEH*, Otilia COSTISOR

Institute of Chemistry Timisoara of Romanian Academy, Bv. Mihai Viteazu, No.24,
RO-300223 Timisoara, Romania;
*e-mail: lili_cseh@yahoo.com

Abstract: *New binuclear $Zn_2(ZOPP\text{-}2H)(CH_3COO)_2$ complex (where ZOPP = N,N'-bis[(4-decyloxy-salicylideneamino)-propyl)-piperazine]) has been synthesized and characterized by elemental analysis, ^1H- NMR, FT-IR, UV-Vis and fluorescence spectroscopy. The non-electrolyte character of the complex was evidenced by conductivity measurement. The zinc ions are penta-coordinated by the N_2O donor sets namely one phenolate oxygen atom, one imine nitrogen and one piperazine nitrogen atoms of Schiff base and two oxygen atoms of the acetate group. The Zn(II) complex displayed fluorescence from the intra-ligand emission excited state in N, N-dimethylformamide (DMF) solution at room temperature. The thermal behaviour of Zn(II) complex and other Ni(ZOPP-2H) complex previously reported suggested a high stability of these compounds compared to ZOPP ligand.*

Keywords: 3d Schiff base complexes; fluorescence; thermal analysis

INTRODUCTION

Schiff base metal complexes have been extensively studied for years due to their selectivity and sensitivity towards the transition metal ions (Hernández-Molina et al. 2004, Andruh et al. 2005). Schiff bases derived from the salicylaldehydes and diamine are known as polydentate ligands with synthetic flexibility, which are often used as chelating ligands in the field of coordination chemistry leading to stable metal complexes (Kuma et al. 1980). Additionally, their 3d metal complexes turned out to be interesting in the fields of liquid crystals (Donnio et al. 1999, Paul et al. 2015), biological such as antimicrobial (Golcu et al. 2005), antibacterial (Chohan et al. 2010, Esmadi et al. 2016) and antifungal agents (Creaven et al. 2010), optoelectronic materials (Hai et al. 2011, Che et al. 2010) and sensors (Gebreyesus et al. 2015, Sakthinathan et al. 2017). Moreover, zinc(II) complexes containing Schiff base ligands are known as fluorescent material or candidates for biological use having intense emission at room temperature (Wen et al. 2012, Qin et al. 2009). Also, thermal behaviour of Schiff base metal complexes has been widely investigated (Ates et al. 2010, Lemos et al. 2004, Durmus et al. 2006, Bartyzel 2017), their metal oxides being used as photoconductors (Mishra et al. 2012), catalysts for a number of reactions like hydrogenation (Osawa et al. 2005), oxidation (Nichio et al. 1996, Abbasi et al. 2014) and decomposition (Deraz et al. 2009, Harraz et al. 2010).

Previously, we reported on the synthesis and characterisation of a new Schiff base ligand (ZOPP) and its coordination complexes with Cu(II) and Ni(II) metal centres (Cretu et al. 2008). In Chart 1 is presented the chemical structure of one of these metal complexes, based on Ni(II) metal centre.

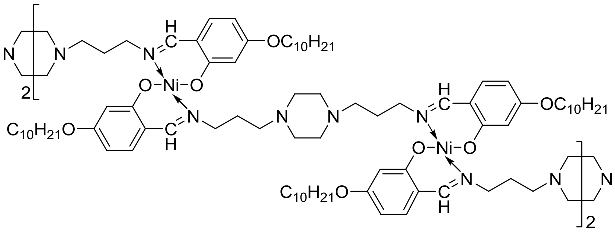

Ni(ZOPP-2H)

Chart 1. Chemical structure of complex **1**

In this paper we present the synthesis and physico-chemical characterization of a new binuclear zinc(II) complex of general formula $Zn_2(ZOPP\text{-}2H)(CH_3COO)_2$ based on the Schiff base ligand ZOPP. Also, the thermal stabilities of the previously reported Ni(ZOPP-2H) (**1**) and the herein synthesised $Zn_2(ZOPP\text{-}2H)(CH_3COO)_2$ (**2**), compared with ZOPP ligand are evaluated.

MATERIALS AND METHODS

Salicylaldehyde and 1,4-bis(3-aminopropyl)-piperazine, were purchased from Sigma Aldrich; zinc(II) and Ni acetate (II) was purchased from Merck. All reagents were of analytical grade and used without further purification. Elemental analysis was carried out on a Perkin Elmer model 240C elemental analyser for C, N, and H and a Flame Atomic Absorption GBC SENSAA Spectrometer. ^{1}H-NMR spectra were run on a Bruker Furier 300 MHz spectrometer. Electronic spectrum was recorded on an Agilent Cary 60 spectrometer. Electric molar conductivity was measured in dimethylformamide solution with a Mettler Toledo FiveEasy plus (FP30) conductivity meter equipped with a Lab. conductivity sensor LE740. Fluorescence spectrum was recorded on freshly prepared solution using a Perkin Elmer LS-55 spectrophotometer; the excitation slit was set at 15 and that of the emission at 5, while the scanning speed was 100 nm/min. IR spectrum was recorded on a Cary 630 FT-IR spectrophotometer, as KBr pellet, in the 400-4000 cm^{-1} range. Thermal analysis curves [thermogravimetric analysis (TGA) and differential thermal analysis (DTA)] were obtained using a TGA/SDTA 851-LF 1100 Mettler Toledo apparatus under the following conditions:

- 25-500 °C, N_2 dynamic atm. at a volumetric flow rate of 50 mL/min. and a heating rate of 10 °C/min.
- 500 °C, N_2 dynamic atm. at a volumetric flow rate of 50 mL/min. and an isothermal heating for 30 minutes under the same dynamic atmosphere.
- 500-900 °C air dynamic atm. at a volumetric flow rate of 50 mL/min. and a heating rate of 10 °C/min.

The air supplied by a compressor (4–5 bar) was passed over granular silica gel. The nitrogen was supplied from Linde gas cylinder (150 bar) of 4.6 purity class.

Synthesis

Schiff base (ZOPP) and Ni(ZOPP-2H) (**1**) were physico-chemical characterized and previously reported (Cretu et al. 2008). Here we discuss only their thermal behaviour in nitrogen – air conditions. The $Zn_2(ZOPP\text{-}2H)(CH_3COO)_2$ (**2**) complex was prepared according to the procedure described in our previous paper (Cretu et al. 2009) using a metal to ligand molar ratio of 2:1.

*Ni(ZOPP-2H) (**1**)*

TG/DTG/DTA (Mass loss %), solid residue of NiO: calcd. 9.60; found: 8.89.

*$Zn_2(ZOPP\text{-}2H)(CH_3COO)_2$ (**2**):* Yield: 78.4 %

Elemental analysis (%) calcd. for $C_{48}H_{76}N_4O_8Zn_2$ (967.91): C 59.56; H 7.91; N 5.79; Zn 13.51; exp. C 59.23; H 8.04; N 5.67; Zn 13.07;

Molar conductivity Λ_M, $\Omega^{-1}mol^{-1}cm^2$ (DMF, 10^{-3}M): 2.1;

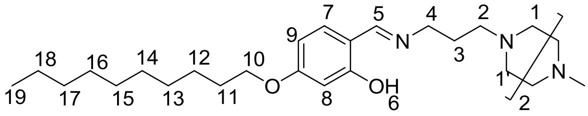

^{1}H-NMR (300 MHz, $CDCl_3$) δ [ppm]: 7.95 (s, 1H, H^5); 6.90 (d, 1H, H^7); 6.31 (d, 1H, H^9); 6.17 (dd, 1H, H^8); 3.90 (t, 4H, $H^{10,4}$); 2.78-3.13 (m, 6H, $H^{1,1',2}$); 2.02 (s, 3H, $CH_{3acetate}$); 1.94 (m, 2H, H^{11}); 1.74 (m, 2H, H^3); 1.27–1.42(m, 14H, H^{12-18}); 0.88 (t, 3H, H^{19});

FT-IR (KBr) ν_{max} [cm^{-1}]: 2925, 2854 $\nu^{as,s}(CH_2)$, 1608 ν(C=N), 1528, 1436, 1400 $\nu^{as,s}(COO^-)$, 1211 ν(C-O), 683, 612 ν(Zn-O), 463 ν(Zn-N);

UV-Vis (DMF, 10^{-4}M) λ [nm] (ε, M^{-1}cm^{-1}): 287 (28500), 351 (21200);

Fluorescence (DMF): λex: 311 nm; λem: 424 nm.

TG/DTG/DTA (Mass loss %)**,** solid residue of 2ZnO**:** calcd. 16.81; found: 16.39.

RESULTS AND DISCUSSIONS

The synthesis of the Zn(II) complex was done by reaction of stoichiometric amount of zinc (II) acetate dihydrate salt with ZOPP in ethanol as given in the Scheme 1.

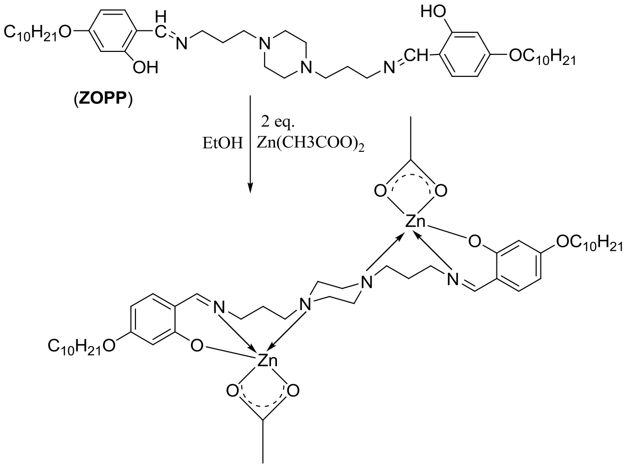

$Zn_2(ZOPP\text{-}2H)(CH_3\text{-}COO)_2$

Scheme 1. The synthesis of complex **2**

The versatile nature of ZOPP allows it to act as bis-bidentate ligand for Ni(II) complex, forming a polymer compound (Chart 1) that usually is obtained when using a metal to ligand molar ratio 1:1, and as bis-tridentate ligand for Zn(II) complex, obtaining a binuclear compound for molar ratio metal to ligand 2:1. In both cases the piperazine bridge adopts a "chair" conformation. The Zn(II) complex structure is proposed by analogy with other similar complex earlier reported (Cretu et al. 2015).

The molar conductivity value at 2.1 $\Omega^{-1}mol^{-1}cm^{2}$ in DMF denotes non-electrolyte behaviour of **2** in this solvent (Geary 1971).

In the ^{1}H-NMR spectrum of **2** a shift of proton signals to lower values compared to its position in the free ligand was observed. Moreover, the signal at 13.92 ppm from the ligand spectrum corresponding to -OH proton is not present in the spectrum of **2**, being consistent with the coordination of the deprotonated ligand (ZOPP) to the metal centers. The methylene protons from acetate group are identified in the ^{1}H-NMR spectrum as sharp signal at 2.02 ppm.

In the FT-IR spectrum of **2** some bands appear shifted compared with the free ligand and some of them disappear as a result of complexation process. Thus, the strong band at 1626 cm^{-1} attributed to azomethine vibration mode υ(C=N) in the spectrum of free ligand is shifted to lower frequency at 1608 cm^{-1} in the spectrum of complex **2**. The absorption bands at 2925 cm^{-1} and 2854 cm^{-1} are assigned to aliphatic $\nu^{as}(CH_2)$ and $\nu^{s}(CH_2)$ group, respectively. The phenolic C-O stretching vibration at 1228 cm^{-1} in ZOPP is shifted at 1211 cm^{-1} for the complex **2** as a result of deprotonation and coordination of phenolic oxygen (Sundararajan et al. 2014). The piperazine >N-CH_2 bands disappeared in the spectrum of complex **2**, phenomenon observed when nitrogen atoms from piperazine are coordinated to metal ion. The medium bands at 1528, 1438 and 1400 cm^{-1} in the spectrum of the Zn(II) complex corresponding to $\nu^{as}(COO^{-})$ and $\nu^{s}(COO^{-})$ of acetate group indicates a bidentate mode of coordination, presenting Δ values significantly less than the ionic values (Nakamoto 1963). Moreover, the vibrational mode δ(OCO) from acetate group have been identified at 682 cm^{-1} for Zn(II) complex. Also, new bands at 612 cm^{-1} and 463 cm^{-1} attributed to ν(M–O) and ν(M–N), respectively were observed.

The absorption spectral data for **2** was obtained in freshly prepared DMF solution and compared with ZOPP spectrum (Figure 1). The complex spectrum shows two absorption peaks at 287 nm and 351 nm that may be assigned to $\pi - \pi^*$ intra-ligand transition.

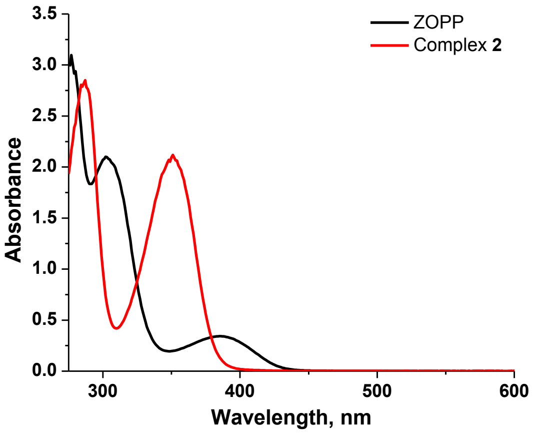

Figure 1. UV-Vis spectra of ZOPP and complex **2** in DMF (10^{-4}M)

The fluorescence spectrum of **2** recorded in DMF solution at room temperature (Figure 2) shows intense fluorescence band usually observed in similar Schiff-base Zn(II) complexes (Pucci et al. 2009), with the emission maximum wavelength at 424 nm attributed to π–π^* singlet ligand-centered excited state. The emission enhancement of

Zn(II) complex is probably due to the chelation effect created through complexation process resulting in increased rigidity of the ligand and thus minimize the loss of energy (Yu et al. 2008).

A blue shift of complex emission compared to ZOPP (λem= 436 nm) was highlighted in the normalized spectrum from Figure 3.

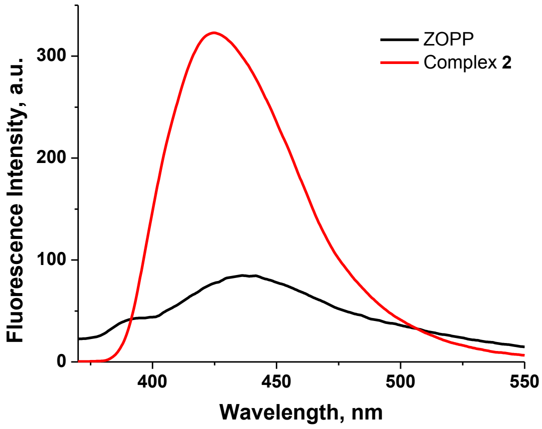

Figure 2. Emission spectra of free ligand and complex **2** in DMF solution

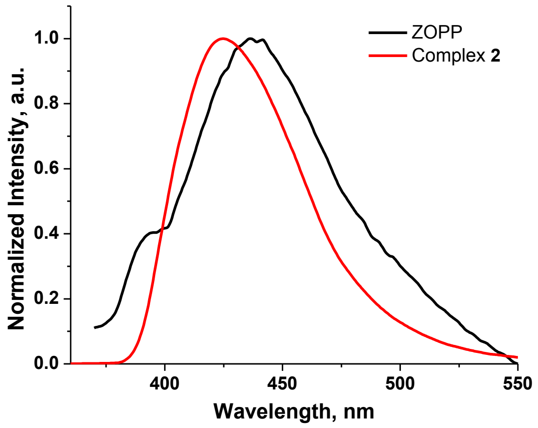

Figure 3. Normalized photoluminescence spectra of free ligand and complex **2**

Thermal behaviour of the complexes (**1** and **2)** and also of their ligand was followed up to 900 ºC under dynamic atmosphere of nitrogen or air and presented characteristic pathways of thermal decomposition, as can be seen from the TG/DTG and DTA curves (Figure 4).

The stages of decomposition, temperature range, decomposition product and weight loss percentage of ZOPP and its complexes are given in Table 1.

Thermal decomposition of the complexes is produced in four steps: two major steps highlighted on DTG curve by intense and well delimited peaks and the other two marked as shoulders. These steps have endo- and exothermic effects on DTA curve.

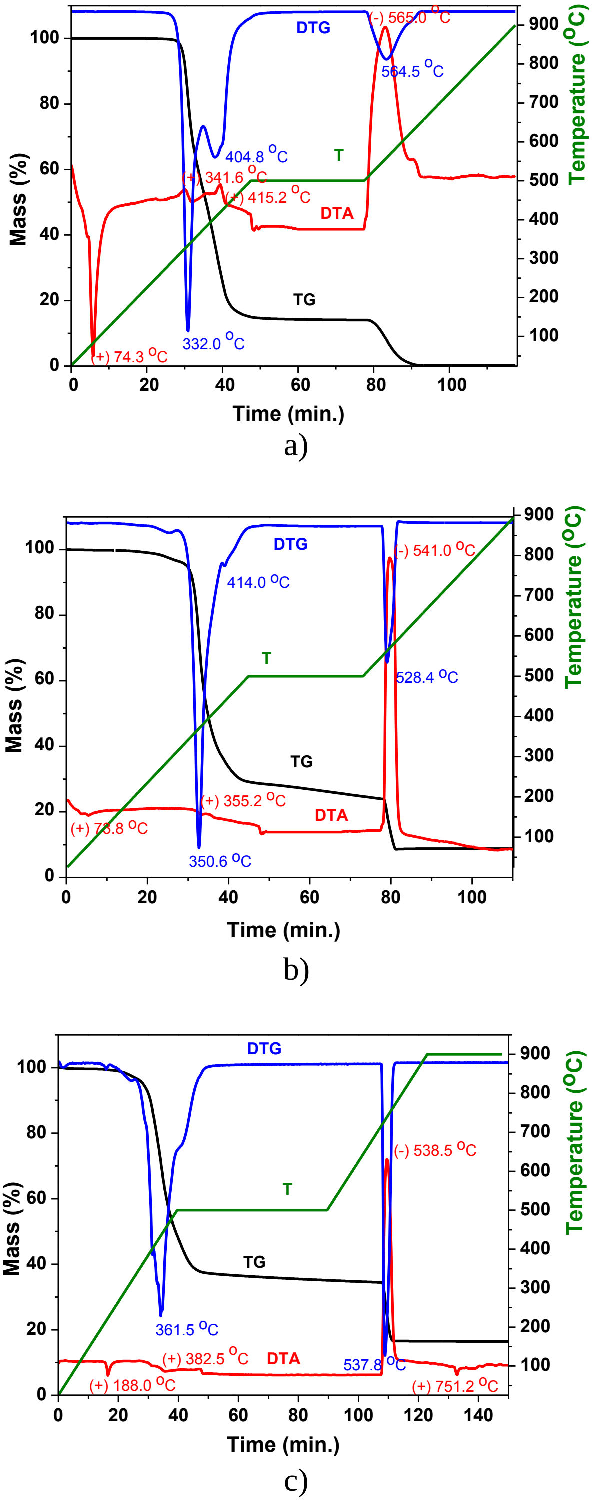

a)

b)

c)

Figure 4. Thermal decomposition of: a) the ligand (ZOPP), b) Ni(ZOPP-2H) and c) Zn_2(ZOPP-2H)(CH_3COO)$_2$ in nitrogen/air condition.

Both **1** and **2** complexes melt at 74 ºC (**1**) and 188 ºC (**2**) then begin to decompose. The first stage of decomposition is in the range 250-300 ºC, the weight loss corresponding to the loss of one or two water from phenolic–OH groups. The second stage of decomposition occurs in the range 300-420 ºC, indicating the loss of piperazine and an organic moiety of the complex with one endothermic DTA peak at 355 ºC (**1**) and 382 ºC (**2**), respectively. The third stage of decomposition in the range 420-500 ºC, is due to loss of two decyl chains of both complexes and two acetate molecules of **2**.

Table 1. The thermal decomposition data for the ligand and its complexes

Comp.	Temp. range (T°C)	Mass loss %		Assignment
		Calcd.	Found	
ZOPP	250-370	46.32^{a}	46.43^{a}	2H_2O from OH, Piperazine, 6CH_2, $C_7H_2N_2O$
	370-500	39.38^{a}	39.53^{a}	2 decyl
	500-900	14.14^{b}	13.78^{b}	C_7H_2O
	Solid residue	0	0	-
1	250-290	2.31^{a}	2.32^{a}	1H_2O from OH
	290-370	36.50^{a}	36.88^{a}	Piperazine, 6CH_2, C_7H_2NO
	370-500	36.50^{a}	36.54^{a}	2decyl
	500-900	17.10^{b}	15.37^{b}	$C_7H_3NO_2$
	Solid residue	9.60^{b}	8.89^{b}	NiO
2	0-300	3.71^{a}	3.21^{a}	2H_2O from OH
	300-420	49.64^{a}	49.56^{a}	Piperazine, 6CH_2, 2decyl, N_2
	420-500	14.88^{a}	12.80^{a}	2Acetate, 2CH
	500-900	18.82^{b}	18.04^{b}	$C_{12}H_2O_2$
	Solid residue	16.81^{b}	16.39^{b}	2ZnO

^{a} - in nitrogen; ^{b} - in air

Further, for a better understanding of the decomposition process, the temperature was maintained at 500°C for 30 min. then the system was supplied with air for complete oxidation of organic residues. A continuous mass loss was observed for **1** and **2** compared with ZOPP where the sample reached constant mass (Figure 4a). The fourth step which occurs at more than 500 ºC is due to loss of other organic moiety and the resulted product were NiO and ZnO with an extremely exothermic DTA peak at 541 ºC and 538 ºC, respectively. A very interesting phenomenon was the melting point at 751 ºC observed in the Figure 5c for complex **2** that is characteristic for ZnO nanorods, greatly reduced comparing with the bulk form (Su et al. 2006). These results of decomposition sub-steps are also identified by IR spectra at 340 and 500 ºC. It is noteworthy that unlike the ligand, mass loss is significantly lower for complexes **1** and **2** in the temperature range of 25-500 °C. This behaviour suggests a high stability of the complexes, the representative mass loss taking place after the temperature of 500 ºC.

CONCLUSIONS

New Zn(II) complex was obtained by direct metal-ligand reaction using 2:1 molar ratio and fully characterized. As results of physico-chemical measurements a discrete binuclear structure was proposed for this complex with a penta-coordinate environment of Zn(II) ions described by the N_2O donor set of Schiff base and two oxygen atoms belonging to the bidentate acetate, the piperazine bridge adopting a "*chair*" conformation. This complex exhibits intense intra-ligand (π–π*) fluorescence in solution. Thermal decomposition of nickel (II) and zinc (II) complexes show four characteristic pathways and higher thermal stability compared with free ligand. The result products in both cases were metal oxides.

ACKNOWLEDGEMENTS

This work was supported by the Romanian Academy, Project 4.1.

REFERENCES

Abbasi, Z., Behzad, M., Ghaffari, A., Rudbari, H.A., Bruno, G., 2014. Mononuclear and dinuclear salen type copper(II) Schiff base complexes: Synthesis, characterization, crystal structures and catalytic epoxidation of cyclooctene. Inorg. Chim. Acta 414, 78-84.

Andruh, M., Tuna, F., in: Cato, M.A. (Ed.) 2005. Focus on Organometallic Chemistry Research, Nova Publishers, Hauppauge, pp. 144-154.

Ates, B.M., Zeybek, B., Aksu, M., Ergun, Ü., Ercan, F., Aksu, M.L., Atakol, O., 2010. Thermal decomposition of new mononuclear Ni(II) complexes with ONNO type reduced Schiff bases and pseudo halogens. Z. Anorg. Allg. Chem. 636, 0000–0000.

Bartyzel, A., 2017. Synthesis, thermal study and some properties of N_2O_4-donor Schiff base and its Mn(III), Co(II), Ni(II), Cu(II) and Zn(II) complexes. J. Therm. Anal. Calorim. 127, 2133-3147.

Che, C.M., Kwok, C.C., Lai, S.W., Rausch, A.F., Finkenzeller, W.J., Zhu, N.Y., Yersin, H., 2010. Photophysical properties and OLED applications of phosphorescent platinum(II) Schiff base complexes. Chem. Eur. J. 16, 233-47.

Chohan, Z.H., Sumrra, S.H., Youssoufi, M.H., Hadda, T.B., 2010. Metal Based Biologically Active Compounds: Design, Synthesis, and Antibacterial/Antifungal/Cytotoxic Properties of Triazole-Derived Schiff Bases and Their Oxovanadium(IV) Complexes. Eur. J. Med. Chem. 45, 2739-2747.

Creaven, B.S., Duff, B., Egan, D.A., Kavanagh, K., Rosair, G., Thangella, V.R., Walsh, M., 2010. Anticancer and antifungal activity of copper(II) complexes of quinolin-2(1H)-one-derived Schiff bases. Inorg. Chim. Acta 363, 4048-4058.

Cretu, C., Cseh, L., Mehl, G.H., Costisor, O., 2008. New compounds with potential liquid crystal properties. Copper(II) and nickel(II) complexes of N,N'-bis(4-decyloxysalicyliden-N-n-propyl)-piperazine. Synthesis and characterization. Mol. Cryst. Liq. Cryst. 481(1), 26-33.

Cretu, C., Bucovicean, C.M., Cseh, L., Mot, C., Mosoarca, E.M., Tudose R., Costisor, O., 2009. Obtaining and characterization of a new Zn(II) complex containing a ligand with piperazine core. New trends and strategies in the chemistry of advanced materials with relevance in biological systems, technique and environmental protection, 5-6 november 2009, Timişoara, Romania, pp. 143-146 (ISSN: 2065-0760).

Cretu, C., Tudose, R., Cseh, L., Linert, W., Halevas, E., Hatzidimitriou, A., Costisor, O., Salifoglou, A., 2015. Schiff base coordination flexibility toward binary cobalt and ternary zinc complex assemblies. The case of the hexadentate ligand N,N'-bis[(2-hydroxybenzilideneamino)-propyl]-piperazine. Polyhedron 85, 48-59.

Deraz, N.M., Selim, M.M., Ramadan, M., 2009. Processing and properties of nanocrystalline Ni and NiO catalysts. Mater. Chem. Phys. 113, 269-275.

Donnio, B., Bruce, D.M., 1999. Metallomesogens. Struct. Bond 95, 193-247.

Durmus, S., Ergun, Ü., Jaud, J.C., Emregül, K.C., Fuess, H., Atakol, O., 2006. Thermal decomposition of some linear trinuclear Schiff base complexes with acetate bridges. J. Therm. Anal. Calorim**.** 86(2), 337-346.

Esmadi, F.T., Khabour, O.F., Abbas, K., Mohammad, A.E., Obeidat, R.T., Mfady, D., 2016. Synthesis, characterization and biological activity of some unsymmetrical Schiff base transition metal complexes. Drug Chem. Toxicol. 39(1), 41-7.

Geary, W.J., 1971. The use of conductivity measurements in organic solvents for the characterization of coordination compounds. Coord. Chem. Rev. 7, 81-122.

Gebreyesus, S.T., Khan, M.A., 2015. An Overview on Metal Complexes of selected Schiff-bases with their Electrochemical and Sensor Aspects. J. Chem. and Chem. Sci. 5(1), 19-27.

Golcu, A., Tumer, M., Demirelli, H., Wheatley, R.A., 2005. Cd(II) and Cu(II) complexes of polydentate Schiff base ligands:synthesis, characterization, properties and biological activity. Inorg. Chim. Acta 358, 1785-1797.

Harraz, F.A., Mohamed, R.M., Shawky, A., Ibrahim, I.A., 2010. Composition and phase control of Ni/NiO nanoparticles for photocatalytic degradation of EDTA. J. Alloys Compd. 508, 133-140.

Hai, Y., Chen, J.-J., Zhao, P., Lv, H., Yu, Y., Xu P., Zhang, J.-L., 2011. Luminescent zinc salen complexes as single and two-photon fluorescence subcellular imaging probes. Chem. Commun 47, 2435-2437.

Hernández-Molina, R., Mederos, A., in: McCleverty, J.A., Meyer, T.J. (Eds.) 2004. Comprehensive Coordination Chemistry II, pp. 411-446.

Kuma, H., Yamada, S., 1980. Synthesis and characterization of metal complexes with Schiff base obtained from N,N'-bis(3-aminopropyl)piperazine and salicylaldehyde derivatives. Bull. Chem. Soc. Jpn. 53, 3218-3220.

Lemos, F.C.D., Muraro, M., Zukerman-Schpector, J., Cavalheiro, É.T.G., Dockal, E.R., 2004. Thermal decomposition of complexes

Manganese(II) and vanadyl with *cis*- and iron(II), manganese(II) and vanadyl with *trans*-n,n'-bis(salicylidene)-1,2-Cyclohexanediamine (salcn). J. Therm. Anal. Calorim**.** 75, 599-606.

Mishra, S.K., Srivastava, R.K., Prakash, S.G., 2012. ZnO nanoparticles: Structural, optical and photoconductivity characteristics. J. Alloys Compd. 539, 1-6.

Nakamoto, K., 1963. Infrared and Raman Spectra of Inorganic and Coordination Compounds, Wiley, New York, pp. 227.

Nichio, N., Casella, M., Ferretti, O., Gonzalez, M., Nicot, C., Moraweck, B., Frety, R., 1996. Partial oxidation of methane to synthesis gas. Behaviour of different Ni supported catalysts. Catal. Lett. 42, 65-72.

Osawa, T., Koganeia, K., Itoa, N., Kitanoa, M., Haradab, T., Takayasu, O., 2005. Study of the properties of nickel oxide and nickel as precursors for the tartaric acid-NaBr-modified nickel catalyst. Catal. Lett. 100, 189-193.

Paul, M.Kr., Singh, Y.D., Singh, N.B., Sarkar U., 2015. Emissive bis-salicylaldiminato Schiff base ligands and their zinc(II) complexes: Synthesis, photophysical properties, mesomorphism and DFT studies. J. Mol. Struct. 1081, 316–328.

Pucci, D., Aiello, I., Bellusci, A., Crispini, A., Ghedini, M., La Deda, M., 2009. Coordination induction of nonlinear molecular shape in mesomorphic and luminescent ZnII complexes based on Salen-like frameworks. Eur. J. Inorg. Chem. 4274-4281.

Qin, D.-D., Yang, Z.-Y., Qi, G.-F., 2009. Synthesis, fluorescence study and biological evaluation of three Zn(II) complexes with Paeonol Schiff base. Spectrochim. Acta A 74, 415-420.

Sakthinathan, S., Chen, S.-M., Liao, W.C., 2017. Multiwalled carbon nanotube supported Schiff base copper complex inorganic nanocomposite for enhanced electrochemical detection of dopamine, Inorg. Chem. Front. 4, 809-819.

Su, X., Zhang, Z., Zhu, M., 2006. Melting and optical properties of ZnO nanorods. Appl. Phys. Lett. 88, 061913.

Sundararajan, M.L., Jeyakumar, T., Anandakumaran, J., Selvan, B.K., 2014. Synthesis of metal complexes involving Schiff base ligand with methylenedioxy moiety: Spectral, thermal, XRD and antimicrobial studies. Spectrochim. Acta A 131, 82-93.

Wen, H.-R., Wang, Y., Chen, J.-L., Tang, Y.-Z., Liao, J.-S., Liu, C.-M., 2012. Syntheses, structures and properties of chiral dinuclear zinc complexes with Schiff-base ligands. Inorg. Chem. Commun. 20, 303-306.

Yu, T., Zhang, K., Zhao, Y., Yang, C., Zhang, H., Qian, L., Fan, D., Dong, W., Chen, L., Qiu, Y., 2008. Synthesis, crystal structure and photoluminescent properties of an aromatic bridged Schiff base ligand and its zinc complex. Inorg. Chim. Acta 361, 233-240.